Journal of Power Sources 244 (2013) 72–79

Contents lists available at SciVerse ScienceDirect

Journal of Power Sources

journal homepage: www.elsevier.com/locate/jpowsour

# Carbon-sphere/$Co_3O_4$ nanocomposite catalysts for effective air electrode in Li/air batteries

Chang Sung Park, Kwan Su Kim, Yong Joon Park*

*Department of Advanced Materials Engineering, Kyonggi University, Suwon, Gyeonggi-do 443-760, Republic of Korea*

## HIGHLIGHTS

- A carbon-sphere/$Co_3O_4$ nanocomposite is introduced as a catalyst for the air electrode.
- $Co_3O_4$ nanoparticles were homogeneously dispersed on the surface of carbon spheres.
- This will increase the carbon/catalyst contact area acting as the catalytic active site.
- The electrode containing carbon-sphere/$Co_3O_4$ nanocomposite showed high capacity.
- It also presented low over-potential, and relatively stable reversibility.

## ARTICLE INFO

*Article history:*
Received 5 November 2012
Received in revised form
24 March 2013
Accepted 25 March 2013
Available online 5 April 2013

*Keywords:*
Lithium air battery
Air electrode
Catalyst
Composite

## ABSTRACT

As a new approach to the development of advanced Li/air batteries, a carbon-sphere/$Co_3O_4$ nanocomposite is introduced as a catalyst for the air electrode. $Co_3O_4$ nanoparticles are dispersed homogeneously on the surface of carbon spheres in an attempt to increase the carbon/catalyst contact area acting as the catalytic active site during the electrochemical reaction. A high discharge capacity, relatively stable reversibility, and low overpotential are observed in electrochemical tests of an electrode containing this carbon-sphere/$Co_3O_4$ nanocomposite. This indicates that the carbon-sphere/$Co_3O_4$ composite is a promising catalyst for the air electrode of Li/air batteries.



## 1. Introduction

Li/air batteries are currently the most promising new rechargeable batteries because they have much higher energy densities than other energy-storage systems such as lithium-ion batteries [1–7]. The high energy density of the Li/air cell is attributed to the fact that the cathode active material (oxygen) is not stored in the battery, but is instead supplied from the environment. Specifically, oxygen is reduced catalytically on an "air electrode" surface, and reacts with the lithium cations supplied by the anode to form $Li_2O_2$ (or $Li_2O$) on the air electrode during the discharge process [8–10]. Theoretically, if oxygen was supplied without limit, the Li/air battery could be discharged until the entire lithium anode had reacted with oxygen. However, in practical applications using organic electrolytes, the energy density of a Li/air cell falls short of the theoretical value. Previous studies have suggested that insoluble reaction products such as lithium peroxide ($Li_2O_2$) may block the catalytic active site, preventing $O_2$ intake and $Li^+$ delivery to the active reaction site and terminating the discharge process [11–13]. Therefore, the practically available capacity of the Li/air battery is highly dependent on the properties of the air electrode. Moreover, the air electrode significantly affects the rechargeability and overpotential of the Li/air cell [8–13].

In general, an air electrode is composed of a catalyst, carbon, and a binder. Although some carbon itself has a catalytic property, this is not typically sufficient to dissociate the reaction products. So it has been known that the oxide catalyst such as $Co_3O_4$ needs for superior catalytic activity of the air electrode. However, the oxide catalysts should be contacted with carbon to compensate for their poor electronic conductivity. Considering the reaction model of the air electrode [12], most active sites may be catalyst/carbon contact areas in the air electrode. Accordingly, it is expected that the use of an air electrode with a wide catalyst/carbon contact area will enhance its catalytic activity. To date, most air electrodes have been

* Corresponding author.
*E-mail addresses:* yjparketri@yahoo.co.kr, yjpark2006@kyonggi.ac.kr (Y.J. Park).

0378-7753/$ – see front matter © 2013 Elsevier B.V. All rights reserved.
http://dx.doi.org/10.1016/j.jpowsour.2013.03.153

prepared by mechanical mixing of carbon with a catalyst [8–10]. However, such mechanical mixing might not disperse a nanosized catalyst perfectly on the carbon surface. Thus, it has been difficult to obtain a sufficient catalyst/carbon contact area.

In the present study, carbon spheres were introduced as a new carbon frame for combination with an oxide catalyst. Our study was motivated by the notion that a carbon sphere with homogeneous surface energy (due to its spherical shape) will facilitate the uniform dispersion and coating of a nanocatalyst on the carbon surface. Thus, the carbon-sphere/catalyst nanocomposite could offer a wide carbon/catalyst contact area, which may act as the catalytic active site. Moreover, the carbon sphere would compensate for the insufficient electronic conductivity of the oxide catalyst. In this work, a carbon-sphere/catalyst composite was fabricated, and its electrochemical properties as the air electrode in a Li/air cell were characterized. $Co_3O_4$ was adopted as the oxide catalyst because of its attractive catalytic activity in various application fields [14–16]. The air electrode containing $Co_3O_4$ has showed high capacity and relatively stable cyclic performance. The carbon-sphere/$Co_3O_4$ nanocomposites are expected to show enhanced catalytic activities as electrode materials for Li/air cells owing to their wide catalytic active areas and improved electronic conductivities.

## 2. Experimental

Carbon-sphere templates were prepared from D-glucose precursors using a modified hydrothermal synthesis process [17,18]. Typically, glucose (3 g) was diluted in deionized (DI) water and mixed by magnetic stirring. The mixture was then sonicated continuously for 10 min until a clear solution was formed. This solution was subsequently transferred to a Teflon-lined stainless-steel autoclave and thermally treated in an electric oven at 180 °C for 14 h. Next, black products were recovered by centrifugation and washed with water and alcohol. Finally, the as-synthesized samples were dried overnight in a vacuum oven at 90 °C. To check the degree of defect of prepared carbon sphere, Raman spectrum was obtained using a Raman spectrometer (Horiba Jobin Yvon, LabRam Aramis).

The carbon-sphere/$Co_3O_4$ nanocomposite was prepared by impregnating carbon spheres with a cobalt nitrate solution, through the dispersion of 2.5 g of carbon spheres in 100 mL of a 0.05 M cobalt nitrate solution under sonication. This mixture was sonicated at room temperature, stirred magnetically for 24 h, and then washed once with water. Subsequently, the powder was dried overnight in an oven at 80 °C, after which it was calcined at 400 °C under a $N_2$ atmosphere. The fabrication process for the composite is shown in Fig. 1. The X-ray diffraction (XRD) patterns of the compound were obtained using a Rigaku X-ray diffractometer with monochromatized Cu-Kα radiation ($\lambda = 1.5406$ Å). The microstructure of the compound was observed using field-emission scanning electron microscopy (SEM, JEOL-JSM 6500F) and transmission electron microscopy (TEM, JEOL-JEM 2100F). The carbon-sphere/$Co_3O_4$ ratio was analyzed using thermogravimetry (TG, STA S-1500) at a scanning rate of 10 °C $min^{-1}$ from 25 to 800 °C in an air atmosphere. The electrochemical performance of an air electrode containing the carbon-sphere/$Co_3O_4$ nanocomposite as a catalyst was examined using a modified Swagelok cell consisting of an air electrode, a metallic lithium anode, a glass filter separator (Whatman), and an electrolyte composed of 1 M LiTFSi in tetraethylene glycol dimethyl ether (TEGDME). The air electrode contained carbon (Ketjenblack (KB) pore volume ≈ 3.21 $cm^3$ $g^{-1}$), the catalyst (carbon-sphere/$Co_3O_4$ nanocomposite, pore volume ≈ 0.038 $cm^3$ $g^{-1}$), and a binder (polyvinylidene difluoride, PVDF). The weight ratio of catalyst/carbon/binder was adjusted to 72:18:10. Because the weight ratio of carbon spheres to $Co_3O_4$ was 71:29 in the composite, the $Co_3O_4$ (oxide catalyst) ratio of the electrode containing the composite was ≈21 wt%.

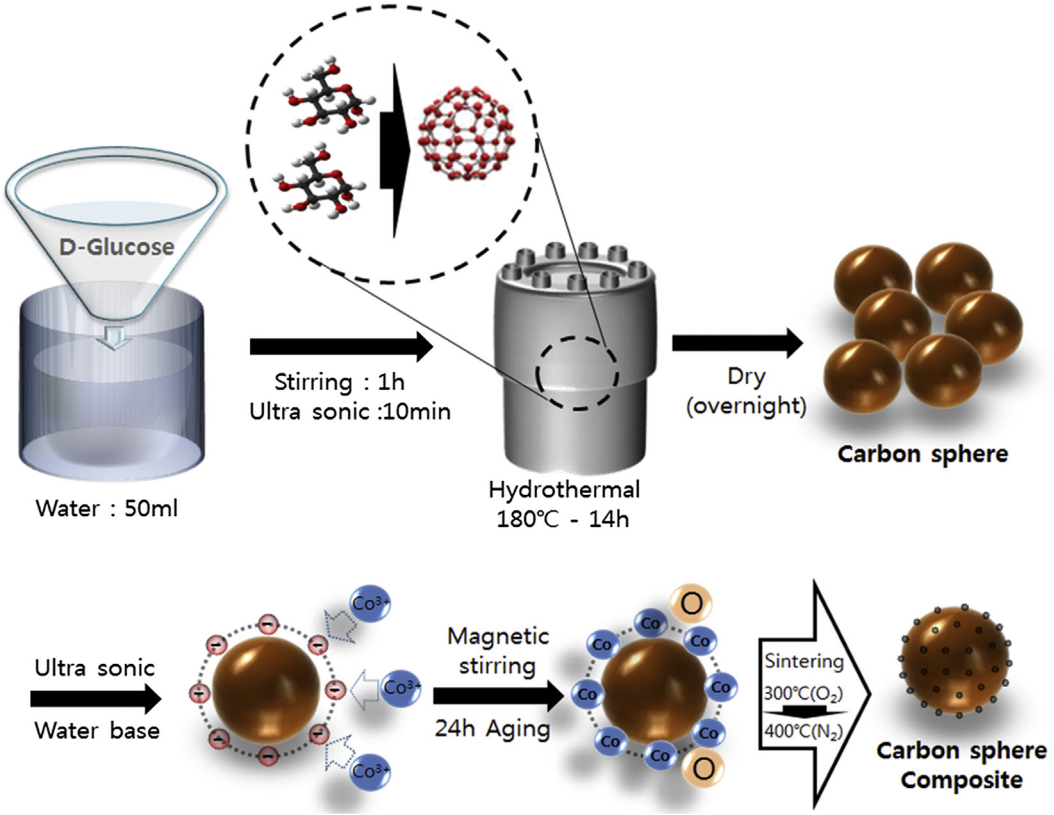


**Fig. 1.** Schematic of the synthetic procedure used to obtain carbon-sphere/$Co_3O_4$ nanocomposite.

An air electrode containing nanosized commercial $Co_3O_4$ powder (Aldrich, average size ≈ 50 nm, pore volume ≈ 0.28 $cm^3\ g^{-1}$) was also prepared with the same $Co_3O_4$/carbon/binder ratio (21:69:10) as the air electrode containing the carbon-sphere/$Co_3O_4$ composite, for comparison of the electrochemical properties of the electrodes. The components were then ball-milled for homogeneous mixing, after which they were coated onto porous carbon paper (JNTC Co.) and dried at 90 °C for 2 h. Several holes were made on one side of a Swagelok cell rod to expose the air electrode to the $O_2$ atmosphere. The cell was then assembled in an Ar-filled glove box and subjected to galvanostatic cycling using a WonAtech (WBCS 3000) charge/discharge system. The experiments were conducted under an $O_2$ pressure of 1 atm in an air chamber.

## 3. Results and discussion

Fig. 2a shows a typical SEM image of a carbon sphere. The carbon spheres have a circular shape and a relatively uniform particle size of approximately 100–300 nm. The size of the carbon spheres could be controlled by the reaction time and temperature, and their surface morphology was smooth and clean, with no heterophase particles. The carbon spheres were heat-treated at low temperature (400 °C) under $N_2$ atmosphere, so they may have many defects. Raman spectroscopy is a widely used technique to check the degree of defect. From the Raman spectrum in Fig. 2b, it can be found that two broad peaks at 1585 $cm^{-1}$ (G band) and 1370 $cm^{-1}$ (D band), which are attributed to amorphous carbon [18]. The peak intensity ratio of D band and G band (D/G) is about 0.58. This is relatively lower than previously reported value for carbon sphere [18], indicating that the degree of defect of the prepared carbon sphere is relatively lower compared to that of typical carbon sphere.

As shown in Fig. 2c, the shape and size of the carbon-sphere/$Co_3O_4$ composite was similar to that of a simple carbon sphere. However, the surface of the composite was rough and covered with nanoparticles. The presence of $Co_3O_4$ nanoparticles on the surface of the carbon spheres was confirmed by scanning electron microscope–energy dispersive spectroscopy (SEM–EDS) analysis. As shown in Fig. 2d, not only C peaks, but also Co peaks were detected during analysis, which implies that the surface of the composite consisted of C and $Co_3O_4$. TEM analysis was conducted to investigate in detail the surface morphologies of the pristine and coated samples. The plain carbon spheres presented a clean surface (Fig. 3a). However, as shown in Fig. 3b–d, the composite surface was dotted homogeneously with nanoparticles of less than 10 nm in size. Homogeneously dispersed nanosized $Co_3O_4$ particles could offer good catalytic efficiency owing to their wide catalytic active area.

The presence of $Co_3O_4$ nanoparticles was also confirmed by X-ray diffraction (XRD). The diffraction pattern of the carbon spheres is shown at the bottom of Fig. 4a. The broad peak centered at approximately $2\theta = 23.5°$ can be indexed as the [002] diffraction peak of turbostratic polyaromatic carbon. The broad graphite peaks indicate the highly disordered structure of the carbon spheres [19]. The top portion of Fig. 4a shows the diffraction peaks for the carbon-sphere/$Co_3O_4$ nanocomposite. Specifically, a broad peak corresponding to the carbon spheres is observed at approximately $2\theta = 23.5°$, and sharp crystalline peaks are also observed. The crystalline peaks can be indexed exactly to a typical $Co_3O_4$ crystalline phase with a spinel structure, which indicates that a $Co_3O_4$ crystalline phase was successfully formed on the surface of the carbon spheres through the hydrothermal method. Fig. 4b presents the XPS spectra of carbon spheres, $Co_3O_4$ commercial powder, and carbon-sphere/$Co_3O_4$ nanocomposite. For the $Co_3O_4$ commercial powder, the peaks due to Co $2P_{3/2}$ and Co $2P_{1/2}$ were observed at binding energy (BE) of 780.0 eV and 795.1 eV, respectively. These values were in good agreement with the reported data for $Co_3O_4$ [20,21]. The spectrum of carbon-sphere/$Co_3O_4$ nanocomposite also showed two major peaks with binding energy values of 781.4 eV

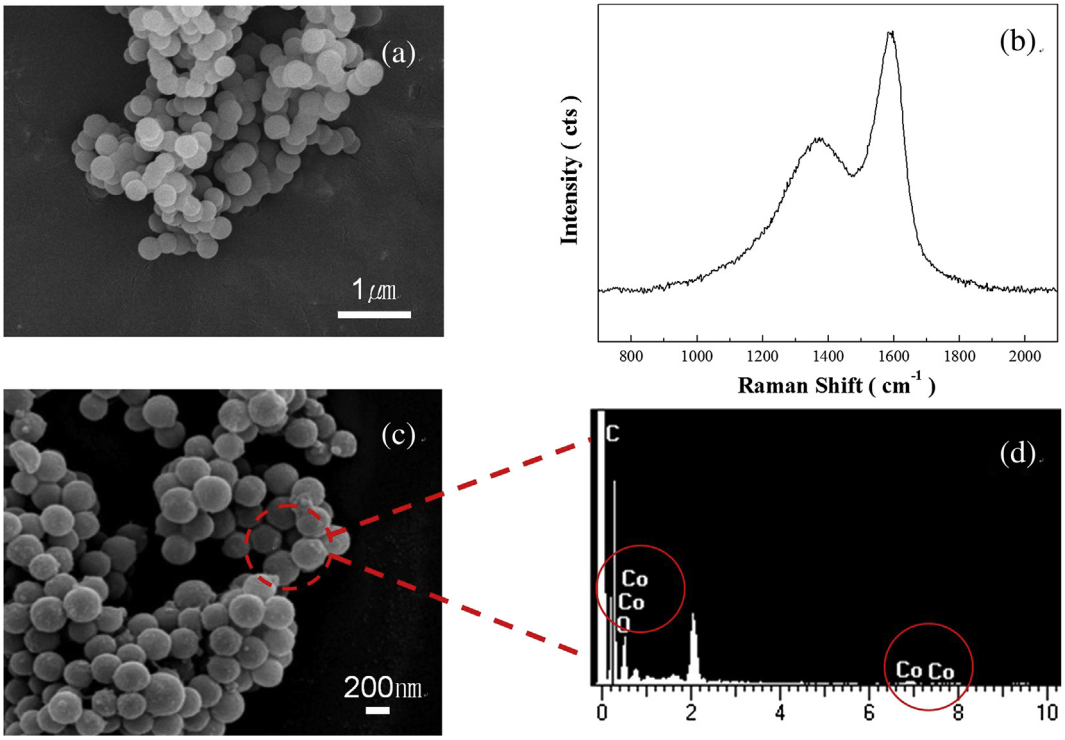


**Fig. 2.** (a) SEM image of the carbon sphere; (b) Raman spectroscopic profile of carbon sphere; (c) SEM image of the carbon-sphere/$Co_3O_4$ nanocomposite; (d) SEM–EDS analysis of the surface of the composite.

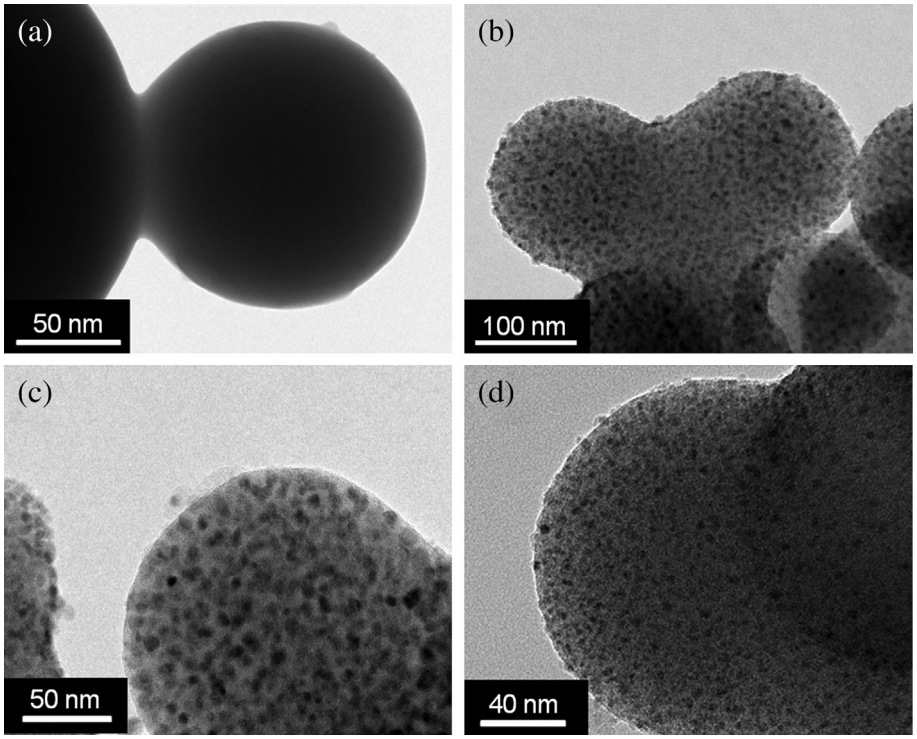


**Fig. 3.** TEM images of the carbon sphere and carbon-sphere/$Co_3O_4$ nanocomposite: (a) carbon sphere, (b), (c), and (d) carbon-sphere/$Co_3O_4$ nanocomposite.

and 797.2 eV, corresponding to Co $2P_{3/2}$ and Co $2P_{1/2}$. Although the peaks was a little shifted to high energy level, the Co $2P_{3/2}$–Co $2P_{1/2}$ peak separation is approximately 15.8 eV, which is comparable to that reported for $Co_3O_4$ indicating the presence of $Co^{2+}$ and $Co^{3+}$ species in the sample. However, several satellite peaks were also observed, which is likely due to binding with carbon. Thermogravimetric (TG) analysis revealed that the weight ratio of the carbon spheres to the $Co_3O_4$ crystalline phase was approximately 71:29, as shown in Fig. 5.

The electrochemical properties of the air electrode containing the carbon-sphere/$Co_3O_4$ nanocomposite were tested to investigate the catalytic activity of the composite in the Li/air cell. The adoption of an appropriate electrolyte is a key factor for obtaining reliable electrochemical behavior. In initial Li/air studies, carbonate-based electrolytes were adopted for the electrochemical tests because they have been used successfully in lithium-ion batteries [8–12]. However, recently, ether-based electrolytes such as TEGDME have been introduced to prevent the easy decomposition of the electrolyte and the formation of lithium carbonate [22–24]. The search for an appropriate electrolyte for the Li/air cell is still underway, but 1 M LiTFSi in TEGDME was adopted as the electrolyte to test our air electrode. The capacity shown in this article is based on the total electrode mass (carbon-sphere/$Co_3O_4$ composite (or catalyst) + carbon + binder), which may be reasonable for the presentation of its energy-storage ability in a rechargeable battery.

Fig. 6a shows the initial discharge/charge profiles of the air electrodes containing the carbon-sphere/$Co_3O_4$ nanocomposite as a function of the loading weight of electrode materials (catalyst + carbon + binder). It is interesting that the specific capacity of the air electrode is highly dependent upon the loading weight. The electrode loaded with 1.1 mg $cm^{-2}$ of "catalyst + carbon + binder" delivered ≈4500 mAh $g^{-1}_{electrode}$ at a constant current density of 200 mA $g^{-1}$ in the voltage range 4.35–2.35 V. However, as the loading weight increased to 1.3 and 1.9 mg $cm^{-2}$, the discharge capacities of the electrodes decreased to ≈3400 and ≈2900 mAh $g^{-1}_{electrode}$, respectively. This implies that the large amount of electrode material per unit area is unfavorable for drawing the full catalytic activity of the electrode. Also, it is not appropriate simply to compare the specific capacities of electrodes with different loading weights (or electrode thicknesses). Therefore, in this work, the loading weight of electrode materials was fixed at 1.3 ± 0.1 mg $cm^{-2}$ to ensure that reliable electrochemical results were obtained.

The initial discharge capacity of the electrode containing the composite was measured at different current densities to characterize the rate capability of the test cell. As shown in Fig. 6b, the initial discharge capacity of the electrode was ≈3400 mAh $g^{-1}_{electrode}$ at a current density of 200 mA $g^{-1}$. However, when the current density was decreased to 100 mA $g^{-1}$, the initial discharge capacity increased dramatically to ≈7000 mAh $g^{-1}_{electrode}$. In contrast, the initial discharge capacity measured at a current density of 400 mA $g^{-1}$ was just ≈2100 mAh $g^{-1}_{electrode}$. This result shows that the capacity of the air electrode is rather sensitive to the current density used for the measurement. The reaction of the air electrode in the Li/air cell (based on an organic electrolyte) on discharging may be suppressed by the formation of solid reaction products. The reaction products covering the surface of the electrode may increase the internal resistance and limit the reaction kinetics of the cell because of their low conductivity, which may lead to a low rate capability of the Li/air cell.

On the basis of the above pre-test, the catalytic activity of the air electrode containing the carbon-sphere/$Co_3O_4$ nanocomposite was compared with those of other air electrodes. Two standard electrodes were prepared for the electrochemical tests. One was prepared using carbon spheres (72 wt% of the total electrode weight) as the catalyst, and with KB carbon (18 wt%) and binder (10 wt%) added in the same amounts as for the electrode containing the carbon-sphere/$Co_3O_4$ nanocomposite. The other was fabricated using simple mixing of commercial nanosized $Co_3O_4$ powder, KB carbon, and binder. The $Co_3O_4$/carbon/binder ratio was adjusted to 21:69:10 because that was the ratio in the electrode containing the

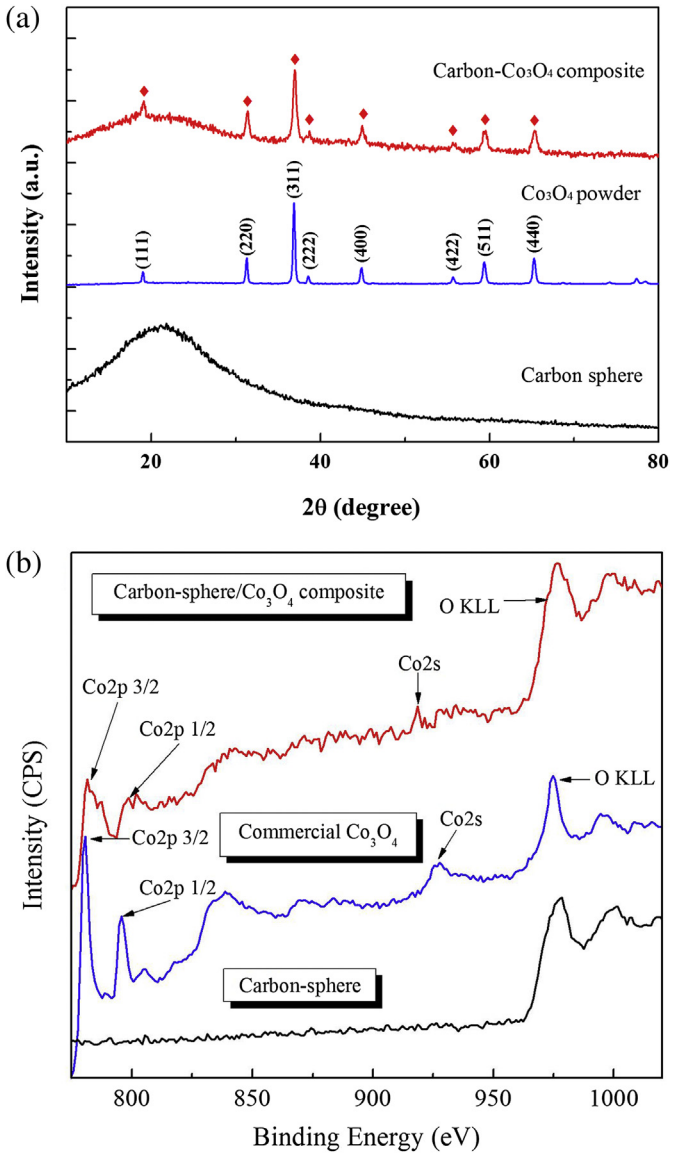


**Fig. 4.** (a) XRD patterns of carbon spheres, $Co_3O_4$ commercial powder, and carbon-sphere/$Co_3O_4$ nanocomposite; (b) XPS spectra of carbon spheres, $Co_3O_4$ commercial powder, and carbon-sphere/$Co_3O_4$ nanocomposite.

carbon-sphere/$Co_3O_4$ nanocomposite. The current density was fixed to 200 mA $g^{-1}$ for this test. Considering that 200 mA $g^{-1}$ is approximately a 1.5–1.6C rate of the cathode containing $LiCoO_2$ in lithium-ion cells, it is a reasonable value to use for the investigation of the commercially available capacity of the air electrode.

Fig. 7 compares the initial discharge/charge profiles of the three different electrodes, measured in the voltage range 4.35–2.35 V (loading weight = 1.3 ± 0.1 mg $cm^{-2}$). It is noticeable that the electrode containing the carbon-sphere/$Co_3O_4$ nanocomposite had a somewhat higher discharge voltage than the other electrodes. Moreover, the charge voltage of the electrode containing the composite was significantly lower than those of the other electrodes. This indicates that the carbon-sphere/$Co_3O_4$ nanocomposite effectively reduced the overpotential (defined as the deviation from the standard potential) of the test cell. The standard potential of the Li/air cell can be calculated from the free energy of each half-cell reaction. However, in practice, the reaction kinetics are suppressed by several limiting factors [25]. On discharging, the

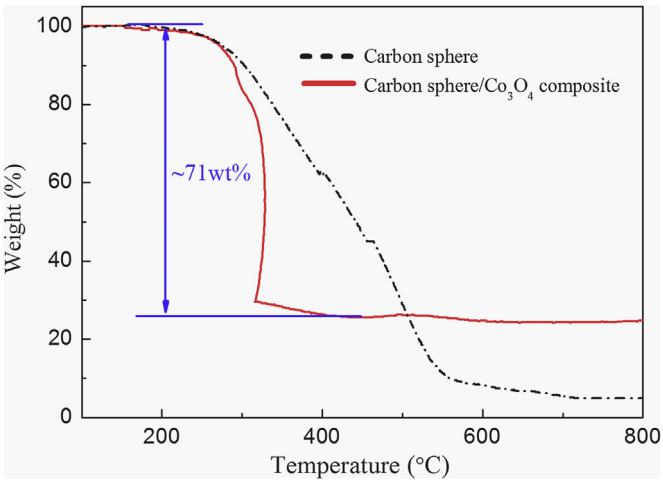


**Fig. 5.** Thermogravimetric (TG) analysis of the carbon sphere and carbon-sphere/$Co_3O_4$ nanocomposite.

formation of reaction products such as $Li_2O_2$ may increase the internal resistance, reduce the reaction kinetics, and require extra energy. So the discharge potential deviates in the negative direction from the standard potential (negative overpotential). On charging, extra energy is required for the decomposition of the reaction products to oxygen and lithium ions, which leads to a positive deviation of the real potential from the standard potential (positive overpotential). In particular, the overpotential on charging is

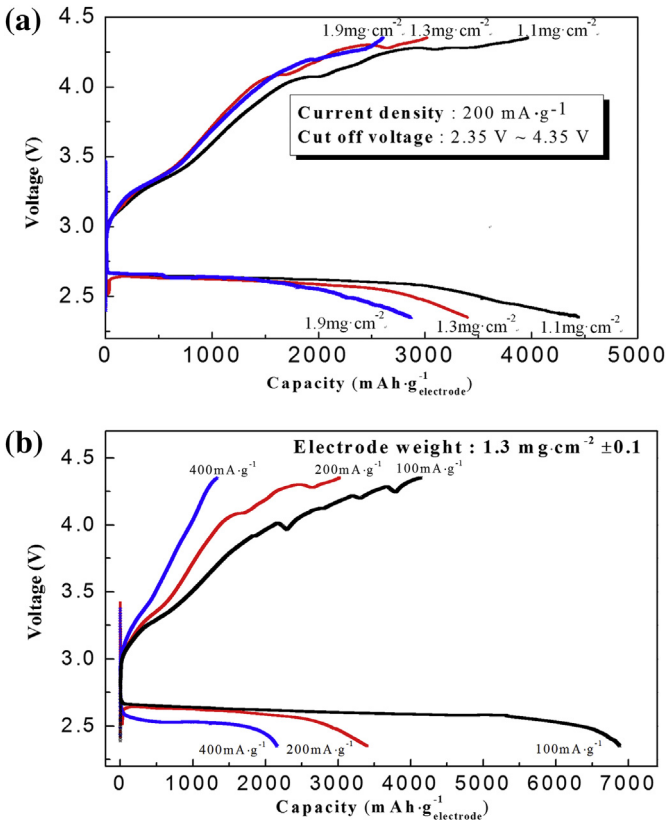


**Fig. 6.** Initial capacity of the air electrode containing carbon-sphere/$Co_3O_4$ nanocomposite measured at a variety of (a) loading weights of electrode materials, and (b) current densities used for the test.

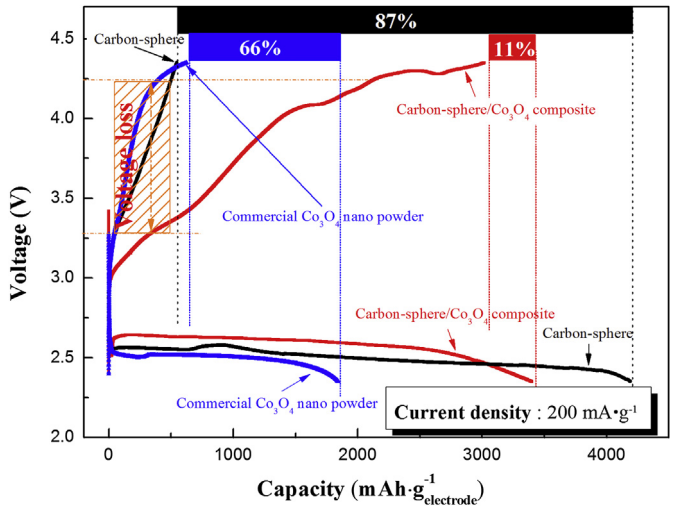


**Fig. 7.** Initial discharge/charge profiles of the air electrodes containing plain carbon spheres, commercial $Co_3O_4$ nanopowder, and the carbon-sphere/$Co_3O_4$ nanocomposite. The voltage range was 4.35–2.35 V and the current density was 200 mA $g^{-1}$ (Top of the figure presents the difference between initial discharge capacity and charge capacity as %).

higher than that on discharging because a lot of extra energy is required for the decomposition of the solid reaction products. The reduced overpotential of the electrode containing the carbon-sphere/$Co_3O_4$ nanocomposite, as shown in Fig. 7, demonstrates the superior catalytic activity of the composite in the charging and discharging processes. In other words, the carbon-sphere/$Co_3O_4$ nanocomposite is an effective catalyst for suppressing the increase in internal resistance due to the formation of reaction products on discharging, and for facilitating the decomposition of reaction products to oxygen and lithium ions on charging. In particular, considering that the reduction in overpotential was more significant for the charging process, it is likely that the extra energy required to drive the decomposition of the reaction products is decreased by the carbon-sphere/$Co_3O_4$ nanocomposite.

In contrast, the electrodes containing carbon spheres and commercial $Co_3O_4$ nanopowder showed higher overpotentials than the composite electrode. The initial discharge capacity of the electrode containing carbon spheres reached ≈4200 mAh $g^{-1}_{electrode}$. This large discharge capacity is attributed to the fact that the carbon spheres are lighter than the $Co_3O_4$ catalyst. However, the overpotential of this electrode was much higher than that of the composite electrode. Moreover, 87% of the initial discharge capacity was lost on charging, so the initial charge capacity was just 13% of the initial discharge capacity, as shown at the top of Fig. 7. Considering that the capacity difference between the initial discharge and charge was just 11% for the composite electrode, it is demonstrated that the carbon spheres themselves do not exhibit good catalytic activity for the decomposition of the reaction products. The electrode containing the commercial $Co_3O_4$ nanopowder also showed a somewhat lower discharge capacity and higher overpotential on initial cycling than the composite electrode, with 66% of the initial discharge capacity lost on initial charging. This electrode was fabricated by simply mixing the $Co_3O_4$ nanopowder and carbon. The nanosized catalysts ($Co_3O_4$) may not be dispersed perfectly, and may be considerably aggregated in the electrode, which may limit the exhibition of their full catalytic activity. On the other hand, with the carbon-sphere/$Co_3O_4$ nanocomposite, the homogeneously dispersed $Co_3O_4$ nanoparticles on the surface of the carbon spheres may offer enough catalytic active sites for the formation and decomposition of reaction products. Moreover, the low electronic conductivity of the $Co_3O_4$ catalyst could be improved by the carbon composition, allowing the complete catalytic nature of the $Co_3O_4$ nanoparticles to be revealed.

Fig. 8 shows the discharge/charge profiles of the three different electrodes (loading weight = 1.3 ± 0.1 mg $cm^{-2}$) in the initial three cycles. As shown in Fig. 8a, the electrode containing the carbon spheres showed a significantly low reversibility, despite its high initial capacity. The capacity dropped almost to zero from the second charging process. The electrode containing the commercial $Co_3O_4$ nanopowder showed a somewhat enhanced reversibility (Fig. 8b). The reversibility of the electrode was clearly improved with use of the carbon-sphere/$Co_3O_4$ nanocomposite as a catalyst for the air electrode (Fig. 8c). However, only ≈25% of the initial discharge capacity remained after three cycles. This rapid capacity fading implies that the reaction products such as $Li_2O_2$ are not perfectly decomposed on charging, and remain on the surface of the electrode. According to previous reports, the charge voltage generally used for cell tests is not sufficient to decompose the reaction products formed after a large depth of discharge [13,25,26]. The cycling test shown in Fig. 8 was attempted with an upper cut-off voltage of 4.35 V to prevent unwanted reactions such as the decomposition of the electrolyte in the high-voltage range.

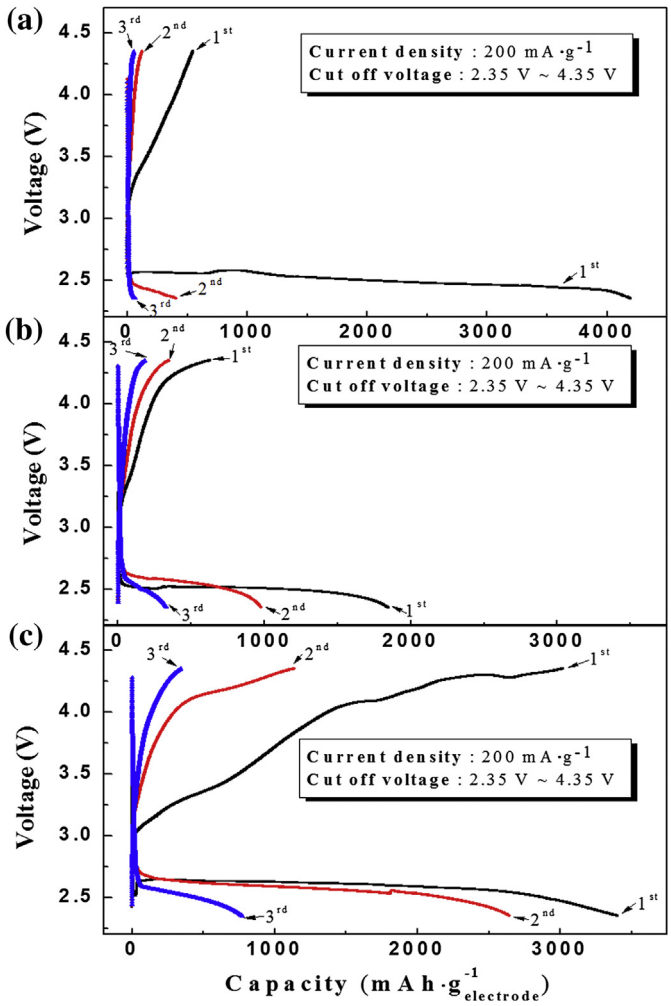


**Fig. 8.** Discharge/charge profiles of the three different electrodes for initial three cycles: (a) electrode containing plain carbon spheres as a catalyst; (b) electrode containing commercial $Co_3O_4$ nanopowder as a catalyst; (c) electrode containing carbon-sphere/$Co_3O_4$ nanocomposite as a catalyst (The voltage range was 4.35–2.35 V and the current density was 200 mA $g^{-1}$).

However, this upper cut-off voltage (4.35 V) is not sufficient for the full decomposition of the reaction products formed on discharging. Moreover, the deep depth of discharge is one of the triggers to deteriorate the air electrode, and the agglomeration of catalyst itself during cycling could be one possibility of the decrease of the catalytic activity of the electrode.

As an approach to avoid a large depth of discharge and obtain an improved cyclic performance of the air cell, the discharge capacity of the electrodes was limited to 1000 mAh $g^{-1}_{electrode}$ (discharge voltage was also limited to 2.0 V). In addition, on charging, after the voltage reached the upper cut-off voltage (4.35 V), the voltage was held at 4.35 V until the current density reached 2 mA $g^{-1}$, which is 1/100 of the current density (200 mA $g^{-1}$), in order to provide enough energy for the decomposition of the reaction products. Fig. 9 shows the discharge/charge profiles of the electrodes measured under the new cycling conditions. The cyclic performances of the electrodes seem to be much improved by the limitation of the discharge capacity and the greater current supply at the fixed voltage. The electrode containing the carbon-sphere/$Co_3O_4$ nanocomposite showed a stable discharge profile up to the 19th cycle (Fig. 9c). However, the average charge voltage gradually increased during cycling, which implies an increase in the internal resistance. The discharge profile of the electrode was shifted considerably to a lower voltage, showing the increase in overpotential on cycling. The gradual increase in overpotential and limited cyclic performance indicates that the reaction products were still not fully decomposed under the new test conditions. It is known that the homogeneous formation of $Li_2O_2$ on discharging and its full decomposition on charging are ideal for a Li/air cell with a good cyclic performance. Some studies have suggested that several reaction products such as $C_3H_6(OCO_2Li)_2$, $Li_2CO_3$, $HCO_2Li$, and $CH_3CO_2Li$ can be formed from the decomposition of carbonate-based electrolytes [13,22,23,27]. These reaction products are not fully dissociated on charging, which lead to a decrease in capacity in successive cycles when using carbonate-based electrolytes. On the other hand, with the TEGDME-based electrolyte used in this work, it has been confirmed that $Li_2O_2$ is formed and decomposed successfully in the initial cycle [22–24]. However, it has also been reported recently that unwanted side reactions still occur on cycling. In particular, $Li_2CO_3$ can be formed through a side reaction at the carbon/$Li_2O_2$ interface after several cycles [28]. The gradual degradation of the electrode containing the composite may be associated with these kinds of side reactions. Previous reports also showed limited cyclic performances over 20 cycles, similarly to that demonstrated in our work [29,30].

The electrodes containing carbon spheres and commercial $Co_3O_4$ nanopowder showed inferior cyclic performances compared with the electrode containing the composite, as shown in Fig. 9a and b. However, it is interesting that the electrode containing the plain carbon spheres showed a relatively stable cycle life. The overpotential of the electrode on charging seemed to be higher than those of the other electrodes containing $Co_3O_4$. However, the supply of more current at a fixed voltage (4.3 V) may be effective for the decomposition reaction and the improvement of the cyclic performance of the carbon-sphere electrode. Fig. 10 shows the cyclic performances of the electrodes under limited capacity (1000 mAh $g^{-1}_{electrode}$) and with the supply of more current at a fixed charge voltage (4.35 V). The electrodes retain their set-up discharge capacity (1000 mAh $g^{-1}_{electrode}$) for 19 cycles (composite electrode), 13 cycles (carbon-sphere electrode), and 7 cycles (commercial $Co_3O_4$ mixture electrode). The superior cyclic performance of the

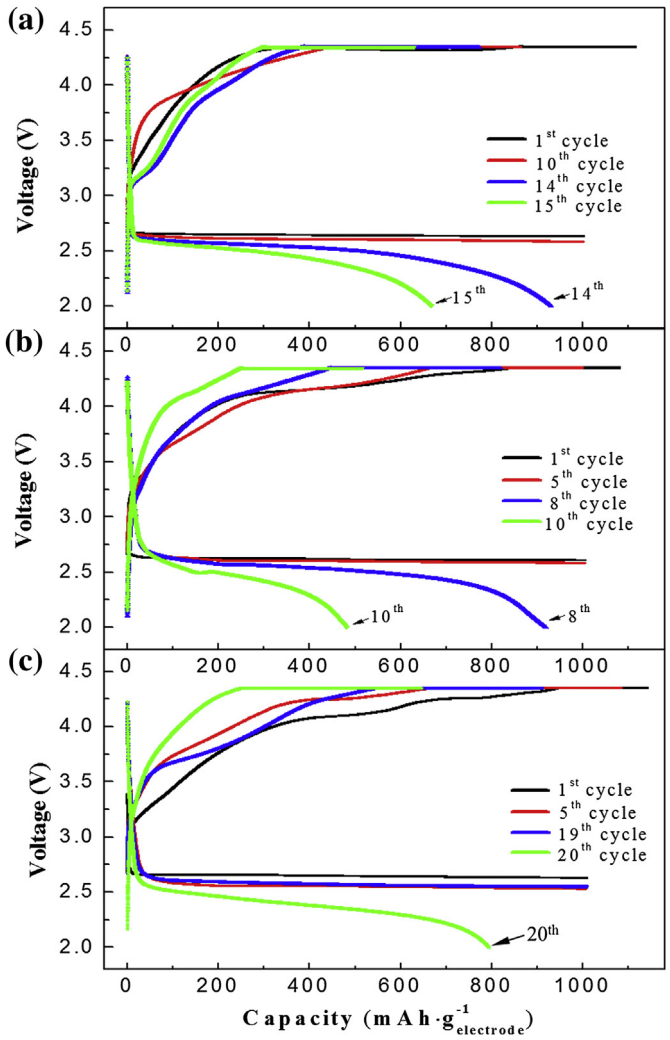


**Fig. 9.** Discharge/charge profiles of the air electrodes measured under limited capacity (1000 mAh $g^{-1}_{electrode}$) and with the supply of more current at a fixed charge voltage (4.35 V): (a) electrode containing plain carbon spheres as a catalyst; (b) electrode containing commercial $Co_3O_4$ nanopowder as a catalyst; (c) electrode containing carbon-sphere/$Co_3O_4$ nanocomposite as a catalyst.

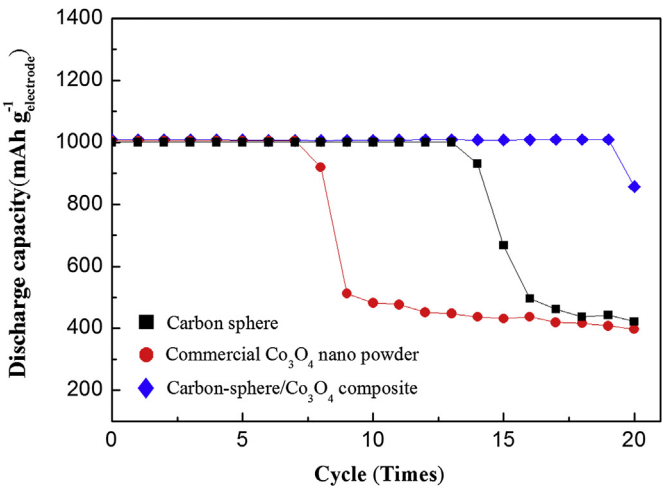


**Fig. 10.** Cyclic performance of the air electrodes measured under limited capacity (1000 mAh $g^{-1}_{electrode}$) and with the supply of more current at a fixed charge voltage (4.35 V).

composite electrode shows that the improved catalytic activity of the composite also enhances the cyclic performance of the air electrode for the Li/air cell. After discharge process, there may exist the following interfaces; i) reaction products/$Co_3O_4$/carbon interface and ii) reaction products/carbon interface in the air electrode. It is easily expected that the reaction products/$Co_3O_4$/carbon interface is more effective to dissociate reaction products such as $Li_2O_2$ than the reaction products/carbon interface. The carbon-sphere/$Co_3O_4$ nanocomposite may have much wider reaction products/$Co_3O_4$/carbon interface, which may facilitate the dissociation of the reaction products and lead to enhanced cyclic performance.

## 4. Conclusions

A carbon-sphere/$Co_3O_4$ nanocomposite was fabricated successfully for use in the air electrodes of Li/air batteries. Carbon spheres (200–300 nm) were dotted homogeneously with ≈10 nm $Co_3O_4$ nanoparticles. The SEM-EDS and XRD patterns confirmed the formation of a $Co_3O_4$ crystalline phase with a spinel structure. The air electrode containing the carbon-sphere/$Co_3O_4$ nanocomposite exhibited a higher capacity and lower overpotential during the discharge/charge process than those containing plain carbon spheres or commercial $Co_3O_4$ nanopowder. These findings indicate that the carbon-sphere/$Co_3O_4$ nanocomposite is a good catalyst for an air electrode with a large catalytic active area. Moreover, the stable contact between the $Co_3O_4$ and the carbon spheres may compensate for the low electronic conductivity of $Co_3O_4$, which may facilitate the achievement of the sufficient catalytic activity of the oxide catalyst.

## Acknowledgment

“This work was supported by the National Research Foundation of Korea Grant funded by the Korean Government (MEST) (NRF-2009-C1AAA001-0094219) and by the Energy Efficiency & Resources of the Korea Institute of Energy Technology Evaluation and Planning (20112010100110) grant funded by the Korea government Ministry of Knowledge Economy”.

## Appendix A. Supplementary data

Supplementary data related to this article can be found at http://dx.doi.org/10.1016/j.jpowsour.2013.03.153.

## References

[1] J. Zhang, W. Xu, W. Liu, J. Power Sources 195 (2010) 7438.
[2] S.S. Zhang, J. Read, J. Power Sources 196 (2011) 2867.
[3] K.M. Abraham, Z. Jiang, J. Electrochem. Soc. 143 (1996) 1.
[4] Y.C. Lu, H.A. Gasteiger, M.C. Parent, V. Chiloyan, S.H. Yang, Electrochem. Solid-State Lett. 13 (2010) A69.
[5] T. Ogasawara, A. Débart, M. Holzapfel, P. Novák, P.G. Bruce, J. Am. Chem. Soc. 128 (2006) 1390.
[6] J.G. Zhang, D. Wang, W. Xu, J. Xiao, R.E. Williford, J. Power Sources 195 (2010) 4332.
[7] Y. Wang, H. Zhou, J. Power Sources 295 (2010) 358.
[8] X.H. Yang, P. He, Y.Y. Xia, Electrochem. Commun. 11 (2009) 1127.
[9] A. Débart, A.J. Paterson, J. Bao, P.G. Bruce, Angew. Chem. 47 (2008) 4521.
[10] F. Jiao, P.G. Bruce, Adv. Mater. 19 (2007) 657.
[11] J. Read, J. Electrochem. Soc. 149 (2002) A1190.
[12] S.S. Zhang, D. Foster, J. Read, J. Power Sources 195 (2010) 1235.
[13] A. Kraytsberg, Y. Ein-Eli, J. Power Sources 196 (2011) 886.
[14] A. Debart, J. Bao, G. Armstrong, P.G. Bruce, J. Power Sources 174 (2007) 1177.
[15] T.H. Yoon, Y.J. Park, Nanoscale Res. Lett. 7 (2012) 28.
[16] K.S. Kim, Y.J. Park, Nanoscale Res. Lett. 7 (2012) 47.
[17] S. Tang, Y. Tang, S. Vongehr, X. Zhao, X. Meng, Appl. Surf. Sci. 255 (2009) 6011.
[18] H. Wang, Q. Dai, Q. Li, J. Yang, X. Zhong, Y. Huang, A. Zhang, Z. Yan, Solid State Ionics 180 (2009) 1429.
[19] Y.F. Shen, P.R. Zerger, N.R. DeGuzman, L.S. Suib, L. McCurdy, I.D. Potter, C.L. O'Young, Science 260 (1993) 511.
[20] C.V. Chenck, J.G. Dillard, J.W. Murray, J. Colloid Interf. Sci. 95 (1983) 398.
[21] M. Oku, Y. Sato, Appl. Surf. Sci. 55 (1992) 37.
[22] C. Laoire, S. Mukerjee, E.J. Plichta, M.A. Hendrickson, K.M. Abraham, J. Electrochem. Soc. 158 (2011) A302.
[23] B.D. McCloskey, D.S. Bethune, R.M. Shelby, G. Girishkumar, A.C. Luntz, J. Phys. Chem. Lett. 2 (2011) 1161.
[24] H.G. Jung, J. Hassoun, J.B. Park, Y.K. Sun, B. Scrosati, Nat. Chem. 4 (2012) 579.
[25] R. Padbury, X. Zhang, J. Power Sources 196 (2011) 4436.
[26] J.S. Lee, S.T. Kim, R. Cao, N.S. Choi, M. Liu, K.T. Lee, J. Cho, Adv. Energy Mater. 1 (2011) 34.
[27] S.A. Freunberger, Y. Chen, Z. Peng, J.M. Griffin, L.J. Hardwick, F. Bard, P. Novak, P.G. Bruce, J. Am. Chem. Soc. 133 (2011) 8040.
[28] B.D. McCloskey, A. Speidel, R. Scheffler, D.C. Miller, V. Viswanathan, J.S. Hummelshøj, J.K. Nørskov, A.C. Luntz, J. Phys. Chem. Lett. 3 (2012) 997.
[29] L.F. Nazar, R. Black, J.H. Lee, B. Adams, A. Baran-Harper, IMLB abstract, 2012, p. S6-2.
[30] S.A. Freunberger, Z. Peng, Y. Chen, P.G. Bruce, IMLB abstract, 2012, p. S6-1.